ac conductivity of mesoscopic rings: The discrete-spectrum limit

B. Reulet and H. Bouchiat
Laboratoire de Physique des Solides, Batiment 510, Université Paris-Sud, 91405 Orsay, France
(Received 20 December 1993)

We present an extensive study of the current response of isolated mesoscopic rings (noninteracting electrons in the diffusive regime) to a small ac flux superimposed on a dc Aharonov-Bohm flux. This response can be very different from the conductance of the same ring connected to a voltage source. We emphasize the importance of the inelastic rate γ compared to the level spacing Δ and the driving frequency ω. We essentially focus on the discrete-spectrum limit $\gamma \ll \Delta$. The conductivity has an imaginary component which, at low frequency, is related to the flux derivative of the persistent current through the ring; as previously shown this quantity presents an ensemble average which is zero in the grand canonical case but which is finite in the canonical statistical ensemble. At frequencies larger than γ we show evidence of an extra contribution to the imaginary conductivity which is finite and temperature independent in the grand canonical ensemble, and increases with temperature in the canonical case. The real part of the average conductivity exhibits $\Phi_0/2$-periodic flux oscillations which are also very sensitive to the statistical ensemble: for the canonical ensemble, these oscillations can assume either sign compared to the Altshuler, Aharonov, and Spivak oscillations observed in long cylinders and connected arrays of rings. We indeed identify different contributions giving rise to flux oscillations of opposite sign. An off-diagonal contribution related to interlevel transitions which is connected with the flux dependence of the level statistics and gives rise to a negative low-field magnetoconductance, and a diagonal contribution related to the flux dependence of the occupation of the different levels. This last quantity is proportional to the average square of the single-level persistent current and to the inelastic scattering time, and gives rise to a positive low-field magnetoconductance. It can be much larger than the Drude conductance. Our results rely on numerical simulations; most of them are also justified analytically.

I. INTRODUCTION

Mesoscopic metallic rings present a spectacular thermodynamic property: they carry a persistent nondissipative current when they are threaded by a magnetic flux.[1–3] This current is a periodic function of the flux, whose periodicity is the flux quantum $\Phi_0 = h/e$; in the presence of disorder giving rise to elastic scattering, its typical value is e/τ_D, where τ_D is the diffusion time of an electron along the circumference of the ring.[4]

The existence of such a persistent current is a consequence of the coherence of the electronic wave functions along the ring, but unlike a superconductor, a mesoscopic ring presents a finite Ohmic conductivity when it is connected to a current source. The average value of this conductivity is given by the Drude formula which reads, in the zero-frequency limit, $\sigma_0 = ne^2\tau_e/m$, where n is the volume concentration of electrons and τ_e the elastic scattering time. Inelastic processes do not appear in this formula; however the sample is implicitly coupled to a thermodynamic reservoir, realized for instance by the macroscopic measuring leads, where the dissipation takes place. Thus the mechanism of dissipation is not intrinsic to the sample.

Such a strong coupling with a reservoir of electrons can be avoided when studying the current response of a mesoscopic ring to a time-dependent flux, which induces an electric field along the ring. This problem was first studied by Büttiker, Imry, and Landauer.[5] They found that the current response to a magnetic flux varying linearly with time (i.e., a constant electromotive force V), presents Bloch like current oscillations of frequency eV/h. An Ohmic-like behavior is recovered only if some inelastic processes are explicitly accounted for, and the conductivity estimated in the linear response limit explicitly depends on these inelastic processes.[6]

One can alternatively study the linear response to a small ac flux superimposed on an Aharonov-Bohm static one. In this case a nondissipative response associated with the flux derivative of the persistent current through the ring is expected. Furthermore, in the presence of inelastic scattering this reactive response is expected to coexist with a dissipative one. This problem has already been addressed in the purely one-dimensional limit by several authors.[7–10] They have pointed out striking differences between the conductivity of an isolated ring and the Drude behavior. In particular, the conductivity explicitly depends on the phenomenological relaxation rate of the electronic-level occupancy probabilities (density matrix) toward equilibrium. Furthermore, the averaged conductivity presents a dc flux dependence which strongly differs from the Altshuler, Aharonov, and Spivak (AAS) oscillations[11] observed experimentally in long cylinders and connected arrays of rings.[12,13] However, the one-dimensional case is very particular, since there is no intermediate regime between the ballistic and the localized one, depending on the circumference of the ring compared to the elastic mean free path.

This is why our aim in this work is to compute the

ac conductivity of a realistic multichannel metallic ring in the diffusive regime $l_e < L < \xi$, where the localization length ξ is approximately equal to Ml_e, and M is the number of transverse channels $Sk_F{}^2/4\pi$. In the one-electron picture such a system is described by an energy spectrum which presents correlations on an energy scale $E_c = hD/L^2$ large compared to the level spacing. A preliminary account of this work is given in Ref. 14. In particular we have emphasized the importance of the parameter γ/Δ where γ is the relaxation rate of the density matrix of the system and Δ the average level spacing. In the continuous-spectrum limit ($\gamma \gg \Delta$) the conductivity at zero frequency is essentially given by the Drude conductivity and exhibits $\Phi_0/2$-periodic flux oscillations of relative amplitude Δ/γ.[11] Differences of the order $(\Delta/\gamma)^2$ between canonical and grand canonical statistical ensembles persisting up to temperatures of the order of E_c have been pointed out.[14,15] In the present paper we focus on the opposite, discrete-spectrum limit ($\gamma \ll \Delta$). Most of the results presented here are based on numerical simulations on the Anderson model; most of them are also justified analytically. They can be summarized as follows:

The real part of the conductivity consists of two pieces: one which involves interlevel processes, $\sigma_{\rm ND}$, and one which involves intralevel processes, σ_D. The average value of $\sigma_{\rm ND}$ exhibits flux oscillations periodic in $\Phi_0/2$ but whose sign is opposite from the AAS oscillations. The relative amplitude of these oscillations, directly related to the change of rigidity of the spectrum induced by the magnetic flux, becomes of the order of unity in the limit $\gamma \ll \Delta$ in the canonical ensemble.

Contrary to $\sigma_{\rm ND}$, which essentially depends on the elastic scattering time τ_e, σ_D is proportional to $1/\gamma$. This quantity is also directly proportional to the average square of the single-level persistent current. In the grand canonical case (and in the canonical case for $T \gg \Delta$), the flux oscillations of σ_D added to the flux-dependent part of $\sigma_{\rm ND}$ give rise to AAS-like oscillations. However, in the limit $\gamma \ll \Delta$ the amplitude of the oscillations of σ_D, which scale like $\sigma_0\Delta/\gamma$, can become very large compared to the Drude conductivity. In the canonical ensemble, the temperature plays a crucial role: σ_D is indeed zero at $T = 0$ and reaches a value which is nearly temperature independent for $T \geq E_c$. This strong temperature dependence does not exist in the grand canonical ensemble. Therefore, in the canonical case at $T = 0$ the total conductivity is given only by the nondiagonal contribution $\sigma_{\rm ND}$. The flux oscillations reverse sign at higher temperature when the diagonal contribution σ_D becomes dominant (the flux oscillations of the total real conductivity at $T = 0$ are of opposite sign for the grand canonical and the canonical statistical ensembles).

The conductivity exhibits an imaginary part which in the low-frequency limit is just proportional to the flux derivative of the persistent current through the ring. In the frequency range $\omega \gg \gamma$, there is an extra diagonal contribution to the imaginary part of the conductivity. This contribution is finite and temperature independent in the grand canonical ensemble, and increases with temperature in the canonical case.

II. THE MODEL

Our study is based on a model already used by Trivedi and Browne[9] for the computation of the conductivity of a one-dimensional (1D) disordered ring driven by an ac electromotive force. Let us first recall this model and point out the underlying assumptions. The ring is described by a one-electron Hamiltonian in the presence of a magnetic flux $\Phi(t) = \Phi_{\rm dc} + \delta\Phi(t)$. If we assume that there is no magnetic field in the ring, the vector potential can be taken orthoradial: $\vec{A}(t) = \vec{A}_0 + \delta\vec{A}(t) = A(t)\vec{e_\theta}$ with the function $A(t)$ uniform through the ring, $A(t) = \Phi(t)/L$. The disorder is described by a potential $V(r,\theta,z)$:

$$H = \frac{1}{2m}[\vec{p} + e\vec{A}(t)]^2 + V(r,\theta,z). \tag{1}$$

The periodic boundary conditions imply $V(r,\theta,z) = V(r,\theta+2\pi,z)$ and $|\Psi(r,\theta,z)\rangle = |\Psi(r,\theta+2\pi,z)\rangle$ for any eigenstate $|\Psi\rangle$ of H.

The disorder is not necessarily small and will not be treated as a perturbation. On the other hand the time-dependent part of the flux is supposed to be sufficiently small compared to Φ_0 to be treated within linear response theory:

$$H = H_0 + \delta H(t) \text{ where } H_0 = \frac{1}{2m}(\vec{p} + e\vec{A_0})^2 + V(r,\theta,z). \tag{2}$$

The eigenstates of H_0 are labeled: $H_0|\alpha\rangle = \epsilon_\alpha|\alpha\rangle$.

Let us now concentrate on the coupling of the system of electrons to an external thermal bath. If the system were completely isolated, the matrix density ρ of the system would evolve according to the Liouville equation

$$i\frac{\partial\rho}{\partial t} = [H,\rho]. \tag{3}$$

In the opposite limit if the electronic gas were instantaneously thermalized its density matrix would be

$$\rho_{\rm equ}(t) = \frac{N\exp[-\beta H(t)]}{Tr\exp[-\beta H(t)]}, \tag{4}$$

where N is the number of electrons in the ring.

In the case of a finite relaxation time, the evolution of the density matrix can be described by a master equation which includes free evolution and relaxation to equilibrium:[16,17]

$$i\frac{\partial\rho}{\partial t} = [H,\rho] - i\gamma(\rho - \rho_{\rm equ}), \tag{5}$$

where γ^{-1} is the relaxation time toward equilibrium. The origin of the existence of γ is the coupling of the sample with a thermal bath (this is done by inelastic scattering of the electrons of the ring). For the sake of simplicity we suppose that γ is temperature independent. If this is not the case, one has to replace γ by $\gamma(T)$ in all results, which can change our conclusions, depending on the mechanism

of thermalization involved in $\gamma(T)$. However, these mechanisms generally have a temperature dependence which is smoother than what we predict for the conductance, so that our results would not be qualitatively altered. Moreover we suppose that γ is energy independent. This could be specially important for $T, \omega \ll \Delta$ where the shape of $\gamma(E)$ could lead to uncontrolled consequences. Let us point out the nontrivial assumption underlying Eq. (5): the equations describing the time evolution of the density matrices of the system and the reservoir can be decoupled, giving rise to an effective evolution equation for the density matrix of the system alone. Moreover, since the coupling with the reservoir is supposed to be weak, its presence affects only the dynamics of the electrons, the static properties remaining unchanged. Hence we are allowed to consider the Hamiltonian of the pure system, and calculate the matrix elements of the operators we consider in the basis of the eigenstates of the pure system. This assumption is correct only if $\gamma \ll \Delta$. An important consequence follows: Since the stationary solution of Eq. (5) is $\rho_{\rm stat} = \rho_{\rm equ}$, all the equilibrium quantities (like the persistent current) are insensitive to the presence of the reservoir.

What remains now is to specify the constraint on the number of particles according to the considered statistical ensemble, canonical or grand canonical. By decomposing the different quantities into their stationary and time-dependent parts, we can write

$$\rho(t) = \rho_0(\Phi_{\rm dc}) + \delta\rho(t)$$
$$\text{with } \rho_0 = \left[\exp\left(\beta(H_0 - \mu_0)\right) + 1\right]^{-1}.$$

In the grand canonical case the chemical potential is considered constant; on the other hand, in the canonical case, where the number of electrons is kept fixed in the system, the chemical potential depends both on time and magnetic flux:

$$\mu(\Phi(t)) = \mu_0(\Phi_{\rm dc}) + \delta\mu(t).$$

The constraint on the number of particles in the system appears at two levels:

(i) For the stationary problem described by H_0, one must have $\mathrm{Tr}\rho_0 = N$ which can be described in terms of an implicit equation allowing one to calculate $\mu_0(N, \Phi_{\rm dc})$:

$$\sum_\alpha f_\alpha = N \text{ with } f_\alpha = \left[\exp\beta(\epsilon_\alpha - \mu_0) + 1\right]^{-1}. \quad (6)$$

(ii) For the time-dependent problem one must have both $\mathrm{Tr}\rho(t) = N$ [equivalent to $\mathrm{Tr}\delta\rho(t) = 0$] and $\mathrm{Tr}\rho_{\rm equ}(t) = N$ with

$$\rho_{\rm equ}(t) = \left[\exp\left(\beta[H(t) - \mu(t)]\right) + 1\right]^{-1}.$$

These two last conditions are equivalent and allow us to calculate $\delta\mu(t)$ in a pertubative way, so that the conductivity can be expressed in terms of the eigenstates and energies of the unperturbed stationary Hamiltonian H_0. As a result, according to Trivedi and Browne,[9]

$$\sigma(\omega) = \sigma_{\rm per} + \sigma_{\rm ND} + \sigma_D \quad (7)$$

$$\text{with } \begin{cases} \sigma_{\rm per} = \dfrac{i}{V}\dfrac{L^2}{\omega}\dfrac{\partial}{\partial\Phi}\displaystyle\sum_\alpha f_\alpha \dfrac{\partial\epsilon_\alpha}{\partial\Phi}, \\ \sigma_{\rm ND} = \dfrac{i}{V}\dfrac{e^2}{m^2}\displaystyle\sum_{\alpha\neq\beta} \dfrac{f_\alpha - f_\beta}{\epsilon_\alpha - \epsilon_\beta}\dfrac{|\langle\alpha|P_\theta|\beta\rangle|^2}{\epsilon_\alpha - \epsilon_\beta - \omega - i\gamma}, \\ \sigma_D = -\dfrac{1}{V}\dfrac{L^2}{\gamma - i\omega}\displaystyle\sum_\alpha \dfrac{\partial f_\alpha}{\partial\Phi}\dfrac{\partial\epsilon_\alpha}{\partial\Phi}, \end{cases} \quad (8)$$

where V denotes the volume of the sample and P_θ the orthoradial component of the kinetic momentum operator $\vec{p}$. Let us now make a few remarks concerning these three terms:

(a) The orbital susceptibility of the persistent current, the first term $\sigma_{\rm per}$ is purely imaginary, i.e., nondissipative, and is directly related to the existence of a finite dc magnetic orbital susceptibility for the ring, $\chi_0 = \lim_{\omega\to 0} \omega\sigma(\omega)$, which is the flux derivative of the persistent current through the ring:

$$I_{\rm per} = -\sum_\alpha f_\alpha \frac{\partial\epsilon_\alpha}{\partial\Phi}. \quad (9)$$

As shown in Refs. 18–23, the grand canonical ensemble average of $I_{\rm per}$ for independent electrons is nearly zero, while it is finite in the canonical ensemble and related to the flux-dependent chemical potential through

$$\langle I_{\rm per}\rangle = \frac{1}{2\Delta}\frac{\partial\delta\mu^2(\Phi)}{\partial\Phi}. \quad (10)$$

In Sec. III, we show that our numerical simulations allow a precise check of this relation. We also study the temperature dependence of the canonical average of the persistent current and of the typical value $\langle I_{\rm per}^2\rangle$ and compare them with the analytical predictions.

(b) The nondiagonal conductivity involves interlevel transitions. In the limit of a continuous spectrum (corresponding either to an infinite system or to a finite disordered system connected to infinite measuring leads), its real part becomes identical to the classical Kubo-Greenwood conductivity, which is the starting point of diagrammatic theory.[11,24–26] *A priori* the ensemble average of $\sigma_{\rm ND}$ contains the Drude conductivity plus weak-localization corrections, which according to AAS[11] give rise to $\Phi_0/2$-periodic flux oscillations. In Sec. IV we present the numerical results we obtained and show that the flux dependence of $\sigma_{\rm ND}$ is always opposite in sign compared to the predictions of weak localization (AAS oscillations); these results can be understood using simple arguments coming from random matrix theory.

(c) The diagonal part of the conductivity, unlike σ_{ND}, does not involve interlevel processes and is directly related to the finite relaxation time of the flux-dependent populations toward equilibrium. σ_D is also related to the presence of the persistent currents through the quantities $\partial\epsilon_\alpha/\partial\Phi$, and so it is only present in the loop geometry. It vanishes in zero flux and for every multiple value of $\Phi_0/2$

and thus gives rise to flux oscillations in the conductivity of the same sign as AAS oscillations. Moreover, unlike σ_{ND}, σ_D goes to zero in the thermodynamic limit. Section V is devoted to the study of this quantity as a function of temperature, which exhibits strong differences in the canonical and grand canonical ensembles.

III. PERSISTENT CURRENT AND TEMPERATURE DEPENDENCE

The persistent current can be decomposed into a Fourier series:

$$I_{\rm per} = \sum_{n=1}^{+\infty} I_n \sin 2n\pi \frac{\Phi}{\Phi_0}, \tag{11}$$

where the I_n are sample-specific quantities. Here we are interested in statistical quantities, the average and the typical current, respectively defined by

$$I_{\rm av} = \langle I_{\rm per} \rangle \qquad I_{\rm typ} = (\langle I_{\rm per}^2 \rangle)^{1/2}. \tag{12}$$

As previously shown the grand canonical average current is nearly zero and the canonical average is finite and $\Phi_0/2$-periodic as a result ($\langle I_{2p+1} \rangle = 0$). Using also the non correlation of harmonics ($\langle I_p I_q \rangle = 0$ if $p \neq q$), the Fourier decomposition of $I_{\rm av}$ and $I_{\rm typ}$ reads

$$I_{\rm av} = \sum_{n=1}^{+\infty} \langle I_{2n} \rangle \sin 4n\pi \frac{\Phi}{\Phi_0},$$
$$I_{\rm typ}^2 = \sum_{n=1}^{+\infty} \langle I_n^2 \rangle \sin^2 2n\pi \frac{\Phi}{\Phi_0}. \tag{13}$$

The flux dependence of $I_{\rm av}$ is shown for different temperatures on Fig. 1. One can note that the strong anharmonicity of the average current observed at low temperature tends to disappear at higher temperature. Note however that the harmonic content of $I_{\rm av}$ does strongly disagree with the results of diagrammatic theory. We come back to this disagreement between the harmonic content of quantities calculated numerically and obtained in diagrammatic theory in Sec. V, when we discuss the flux dependence of the typical level current. On the other hand, nonperturbative calculations (supersymmetry)[28] yield a harmonic content for the average current quite in agreement with our result.[27]

The average and typical current are calculated from the flux-dependent energy spectrum and chemical potential (see Appendix A) for a fixed number of electrons N, following Eqs. (6) and (9), and then averaged over N. At the same time, it was also possible to check the formula derived in Ref. 22 relating the average current to the flux dependence of the chemical potential, which reads:

$$I_{av}(T,\Phi) = \frac{1}{2\Delta} \frac{\partial}{\partial \Phi} \langle [\mu(N,T,\Phi) - \bar{\mu}(N,T)]^2 \rangle, \tag{14}$$

where $\bar{\mu}(N,T)$ is the flux-averaged chemical potential. We find indeed that this quantity coincides remarkably well with the genuine average persistent current, except for temperatures smaller than the level spacing, where it gives rise to slightly less anharmonicity. But at higher temperature the equality of the two quantities is perfect.

Let us now examine the temperature dependence of the average and typical currents: Fig. 2 presents the first terms of the Fourier expansion of $I_{\rm av}$ and $I_{\rm typ}^2$ on a large temperature scale. $\langle I_1^2 \rangle$ and $\langle I_2 \rangle$ both display the same behavior: an exponential decay for $T > E_c$ and

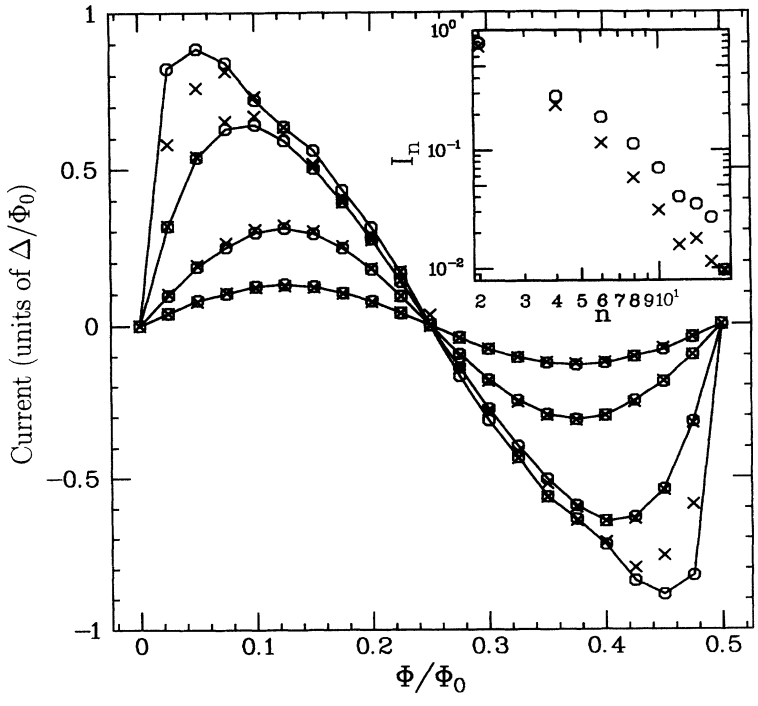

FIG. 1. Average persistent current calculated from numerical simulations on the Anderson model (see Appendix A) for different temperatures ($T/\Delta = 0, 1, 5, 10$). The sample chosen ($64 \times 8 \times 8$, $W = 1.4$) has a Thouless energy estimated to 20Δ (see Appendix B). Crosses correspond to Eq. (14); circles to Eq. (9). One finds a small difference between them at very low temperature, and the higher the temperature, the better the agreement. Inset: harmonic decomposition of these two quantities at zero temperature [the theoretical prediction is I_{2n} constant up to $(E_c/\Delta)^{1/2}$].

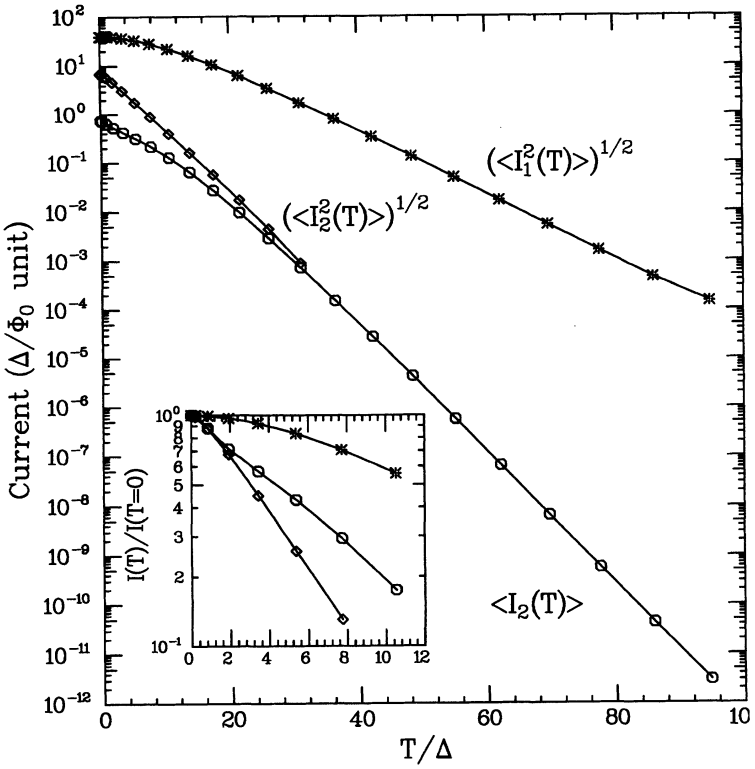

FIG. 2. Temperature dependence of average and typical persistent currents; the sample size and disorder is identical with Fig. 1 Inset: temperature dependence of the same quantities normalized to unity at zero temperature.

a slower decay below E_c. The characteristic temperatures of the high-temperature exponential decay are the following (see Fig. 2):

$$\begin{aligned}&\sqrt{\langle I_1^2(T)\rangle} \propto \exp(-T/T^*),\\ &\langle I_2(T)\rangle \propto \exp(-2T/T^*),\\ &\sqrt{\langle I_2^2(T)\rangle} \propto \exp(-2T/T^*),\end{aligned} \tag{15}$$

where T^* is of the order of $E_c/3$ (see Appendix B for the determination of E_c from our numerical results.) These expressions are significantly different from the diagrammatic calculation results[29] where the high-temperature expansion of the typical squared current is predicted to vary like

$$\langle I_p^2\rangle \propto T^2 \exp(-2\pi pL/L_T) \propto T^2 \exp(-\sqrt{T/T^*}). \tag{16}$$

More precisely, we tried to fit our results with the whole analytical expressions of Ref. 29 but we did not succeed in finding a value of E_c which would be suitable for the whole range of temperature for $I_{\rm typ}$.

Although the average current is not really exponential at low temperature, one can force an exponential fit in order to compare our results with experimental data.[1] If we restrict this fit to the first decade of $I_{\rm av}$, the only measurable part, one obtains a characteristic temperature of T^* (instead of $T^*/2$ in the high-temperature regime, see Fig. 2), i.e., $E_c/3$, to be compared to the experimentally determined value $E_c/2$.[1] Let us emphasize that the temperature dependence we find is much slower than the prediction of the diagrammatic calculation given in Ref. 23, which leads to $T^* = E_c/9$.[30] As a consequence, the discrepancy concerning the temperature dependence of the average current between the one-electron and interacting-electrons pictures is not so important as claimed in Ref. 30.

IV. NONDIAGONAL CONDUCTIVITY

A. Zero temperature

One can see on Fig. 3 the frequency dependence of both imaginary and real parts of the average nondiagonal conductance $\langle g_{\rm ND}\rangle = (S/L)(2\pi h/e^2)\langle\sigma_{\rm ND}\rangle = 2\pi\langle G_{\rm ND}\rangle e^2/h$. One can distinguish on this figure the important characteristic frequency scales: the Thouless energy below which the conductance exhibits a flux dependence estimated to be $E_c = 5\Delta$ (see Appendix B), and the inverse elastic scattering time $h/\tau_e \simeq 20$ above which the real part of the conductance decays like $1/\omega^2$. Note that for frequencies below E_c the imaginary part of the nondiagonal conductance is negligible compared to the real part. In the following we will mainly focus on the real part of $\sigma_{\rm ND}$ which reads

$$\Re(\sigma_{\rm ND}) = \frac{e^2}{m^2 V}\sum_{\alpha\neq\beta}\frac{f_\alpha - f_\beta}{\epsilon_\alpha - \epsilon_\beta}\frac{|\langle\alpha|P_\theta|\beta\rangle|^2\gamma}{(\epsilon_\alpha - \epsilon_\beta - \omega)^2 + \gamma^2}. \tag{17}$$

Our numerical results for the flux dependence of the real part of $g_{\rm ND}$ (in the following we will identify $g_{\rm ND}$ with its real part) at zero frequency and zero temperature are depicted in Fig. 4 for different values of γ. It is also im-

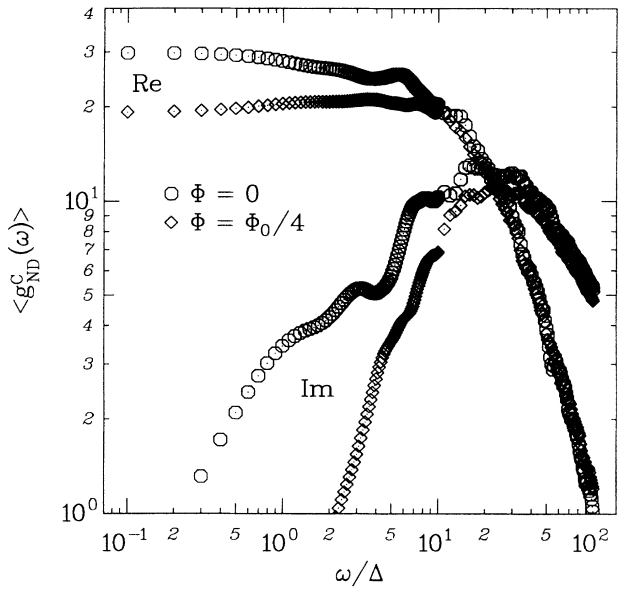

FIG. 3. Frequency dependence of the real and imaginary part of the nondiagonal conductance expressed in units of $e^2/2\pi h$ for the canonical ensemble and $\gamma = \Delta$. These results are obtained from numerical simulations on the Anderson model on a $30 \times 4 \times 4$ ring with disorder $W = 2$; the conductance is averaged over the number of particles between 1/4 and 3/4 filling.

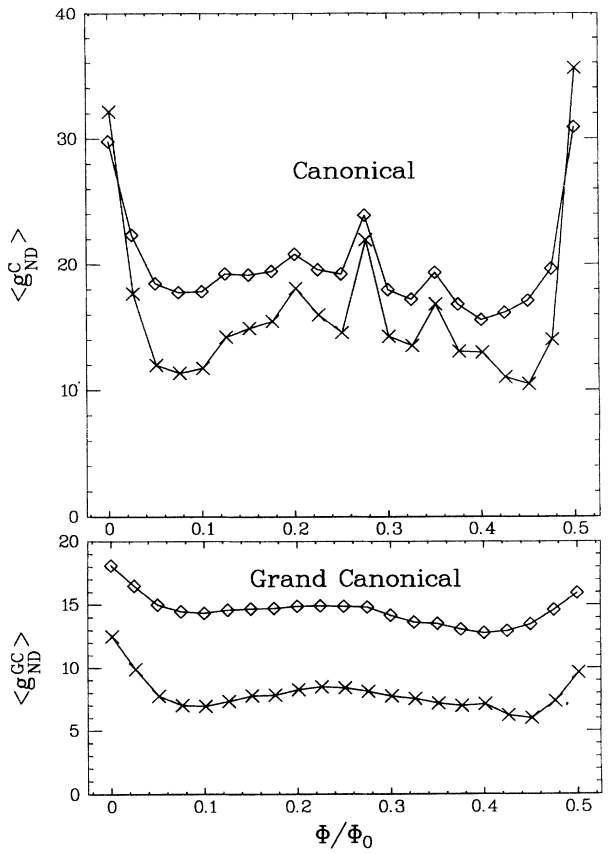

FIG. 4. Flux dependence of the nondiagonal conductance, expressed in units of $e^2/2\pi h$, for the canonical and the grand canonical statistical ensembles, at zero frequency for two different values of γ: $\diamond$, $\gamma = 1$; $\times$, $\gamma = 0.3$. These results are obtained from numerical simulations on the Anderson model on a $30 \times 4 \times 4$ ring with disorder $W = 2$; they are averaged respectively on the number of particles and on the chemical potential between 1/4 filling and 3/4 filling for two different disorder configurations.

portant here to distinguish between canonical and grand canonical averages. In both cases the flux dependence of $\langle g_{\rm ND}\rangle$ exhibits flux maxima at multiple values of $\Phi_0/2$ (which is its periodicity); these maxima become sharper when γ gets smaller and they are more pronounced in the canonical than in the grand canonical case.

Following Gor'kov and Eliashberg[31] and Shklovskii[32] we show that this behavior is a direct consequence of the transition between orthogonal and unitary statistics for the energy-level spectrum. We assume that matrix elements $|\langle\alpha|P_\theta|\beta\rangle|^2 = |P_{\alpha,\beta}|^2$ are independent of α and β, and equal to $|P|^2$.[33] According to our numerical results (see Fig. 16 below), this is a reasonable assumption when $\epsilon_\alpha - \epsilon_\beta$ is smaller than the Thouless energy. [Note that this assumption is quite different from the ansatz of Refs. 31, 35, and 36 which stated that the matrix element $|X_{\alpha\beta}|^2 = |P_{\alpha,\beta}|^2/(\epsilon_\alpha - \epsilon_\beta)^2$ was independent of $\epsilon_\alpha - \epsilon_\beta$. This is due to the difference between the open boundary conditions of their problem compared to the periodic boundary conditions of ours.] It is then possible to write $\sigma_{\rm ND}$ in terms of the function $R(s)$, which is the probability function to have two levels separated by energy s in the spectrum. When performing a grand canonical average we can use the fact that $\langle f_\alpha - f_\beta\rangle_\mu = (\epsilon_\alpha - \epsilon_\beta)/\Delta\mu$ where $\Delta\mu$ is the range of averaging of the chemical potential; as a result,

$$\langle\sigma_{\rm ND}^{\rm GC}\rangle = \frac{|P|^2}{\Delta}\int \frac{R(s)}{\gamma + i(\omega - s)}ds. \tag{18}$$

On the other hand, when performing a canonical average, as already noted, by Shklovskii,[32] $\langle f_\alpha - f_\beta\rangle_N = (\alpha-\beta)/\Delta N$, and the energy denominator does not disappear in the expression for the conductivity, which reads

$$\langle\sigma_{\rm ND}^{C}\rangle = |P|^2\int \frac{R(s)}{s[\gamma + i(\omega - s)]}ds. \tag{19}$$

According to random matrix theory,[34] the small-argument expansion of $R(s)$ reads

$$R(s) = s^\beta, \tag{20}$$

where $\beta = 1$ (2) in the orthogonal (unitary) ensembles corresponding to $\Phi = 0$ $[\Phi_0\sqrt{\frac{\Delta}{E_c}} \le \Phi \le \Phi_0(\frac{1}{2} - \sqrt{\frac{\Delta}{E_c}})$ modulo $\Phi_0/2]$.[37] At $T = 0$ the results for the real part of $\sigma_{\rm ND}$ are:

(i) For the grand canonical case

$$\omega \ll \gamma \begin{cases} \langle\sigma_{\rm ND}^{\rm GC}\rangle(\Phi = 0) \propto \sigma_0(\gamma/\Delta)\log_{10}(\Delta/\gamma), \\ \langle\sigma_{\rm ND}^{\rm GC}\rangle(\Phi = \Phi_0/4) \propto \sigma_0\gamma/\Delta, \end{cases} \tag{21}$$

$$\Delta \gg \omega \gg \gamma \begin{cases} \langle\sigma_{\rm ND}^{\rm GC}\rangle(\Phi = 0) \propto \sigma_0(\omega/\Delta), \\ \langle\sigma_{\rm ND}^{\rm GC}\rangle(\Phi = \Phi_0/4) \propto \sigma_0\omega^2/\Delta^2. \end{cases} \tag{22}$$

(ii) For the canonical case,

$$\omega \ll \gamma \begin{cases} \langle \sigma^C_{\rm ND} \rangle (\Phi = 0) \propto \sigma_0, \\ \langle \sigma^C_{\rm ND} \rangle (\Phi = \Phi_0/4) \propto \sigma_0 (\gamma/\Delta) \log_{10}(\Delta/\gamma), \end{cases} \tag{23}$$

$$\Delta \gg \omega \gg \gamma \begin{cases} \langle \sigma^C_{ND} \rangle (\Phi = 0) \propto \sigma_0, \\ \langle \sigma^C_{\rm ND} \rangle (\Phi = \Phi_0/4) \propto \sigma_0 (\omega/\Delta). \end{cases} \tag{24}$$

We give in Ref. 14 a more precise determination of these expressions using the analytical expression for $R(s)$.[38]

These formulas are strictly valid only in the limit where $\gamma \ll \Delta$; they yield a conductivity in the limit $\omega \gg \Delta$ which is smaller in the grand canonical case than in the canonical one by a ratio of the order of ω/Δ; note also that the quantity $\lim_{\omega,\gamma\to 0} \langle \sigma^C_{\rm ND} \rangle (\Phi = 0)$ is finite. In both cases the flux dependence of the conductivity gives rise to oscillation which are opposite in sign from the AAS ones. Our numerical simulations results displayed in Fig. 5 are in reasonable agreement with these expressions, in the limit where $\gamma, \omega \leq \Delta$. If one then considers the range of frequency where $\omega \geq \Delta$, from Fig. 5 it is possible to see that differences between canonical and grand canonical statistical ensembles tend to disappear at frequencies larger than E_c when the flux dependence of the conductivity becomes negligible .

Concerning now the γ dependence of $\langle g_{\rm ND} \rangle$ at zero frequency, surprisingly one can note on Fig. 6 that, for large values of γ, $\langle g_{\rm ND} \rangle (\Phi = \Phi_0/4)$ is always smaller than $\langle g_{\rm ND} \rangle (\Phi = 0)$ (negative magnetoconductance) in both canonical and grand canonical statistical ensembles. One would expect indeed to recover in the limit $\Delta \ll \gamma \ll E_c$ the results of the diagrammatic theory which exhibits a positive low-field magnetoconductance (AAS oscillations). We understand this disagreement as a consequence of the approximation we used when computing the matrix elements $P_{\alpha,\beta}$ from the eigenstates of the pure system i.e. neglecting the coupling with the thermal reservoir. We already pointed out that this approximation is only valid in the limit where $\gamma \ll \Delta$. If this condition is not fulfilled, one has to calculate the matrix elements of P in the basis of the eigenvectors of the system perturbated by the reservoir. This results in a mixing of $\langle \sigma_{\rm ND} \rangle$ with $\langle \sigma_D \rangle$, which gives rise to AAS-like oscillations. We show indeed in Sec. V that $\langle \sigma_D \rangle$ leads to a positive magnetoconductance.

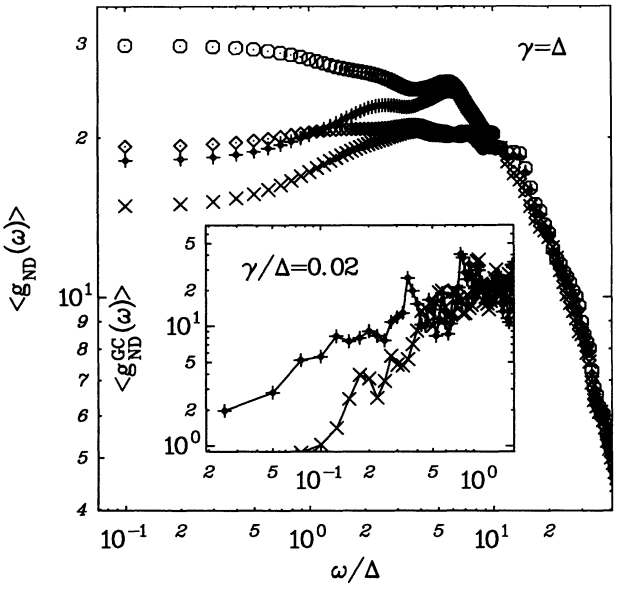

FIG. 5. Frequency dependence of the real part of the nondiagonal conductance expressed in $e^2/2\pi h$ for $\gamma = \Delta$. The canonical statistical ensemble: $\odot$, $\Phi = 0$; $\diamond$, $\Phi = \Phi_0/4$. The grand canonical statistical ensemble: $+$, $\Phi = 0$; $\times$, $\Phi = \Phi_0/4$. Note that for all cases these quantities are frequency independent below $\omega = \gamma = \Delta$. The inset shows the same quantities for $\gamma = 0.02$ and the grand canonical ensemble. In this case the ω and ω^2 dependences predicted from random matrix theory [expression (21)] are clearly observed for the low-frequency conductance at $\Phi = 0$ and $\Phi = \Phi_0/4$. The sample studied and the range of averaging is the same as for Fig. 3.

B. Temperature dependence

The temperature dependence of the oscillating part of the conductance in the canonical ensemble $\delta g_{\rm ND}(T)$ is depicted in Fig. 7 for different values of γ. $\delta g_{\rm ND}(T)$ decreases with temperature until it reaches the grand canonical value. One can clearly distinguish two different regimes in the temperature dependence of $\delta g_{\rm ND}(T)$. For values of γ smaller than Δ, there is a sharp decrease at temperatures below Δ which can be approximately de-

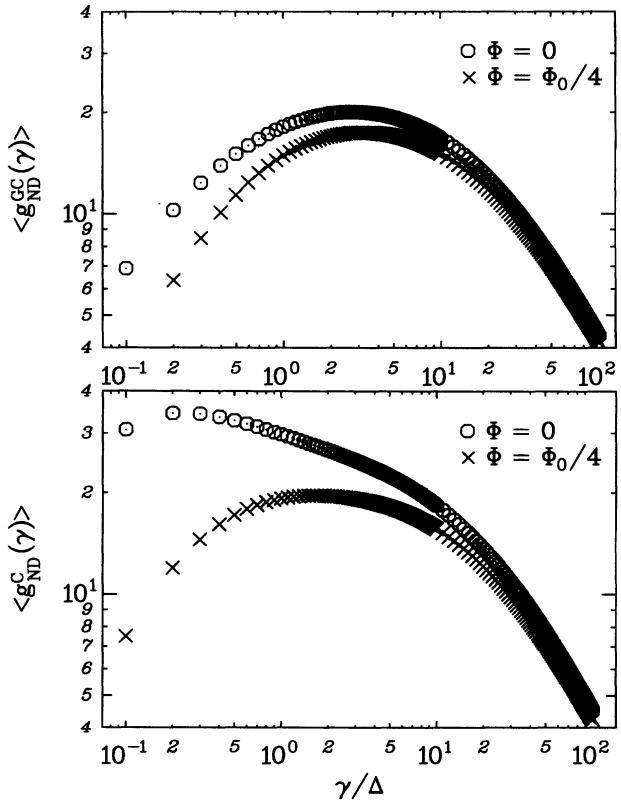

FIG. 6. γ dependence of the real part of the nondiagonal conductance at zero frequency expressed in units of $e^2/2\pi h$, for the grand canonical and canonical statistical ensembles. The sample studied and the range of averaging are the same as for Figs. 3 and 5.

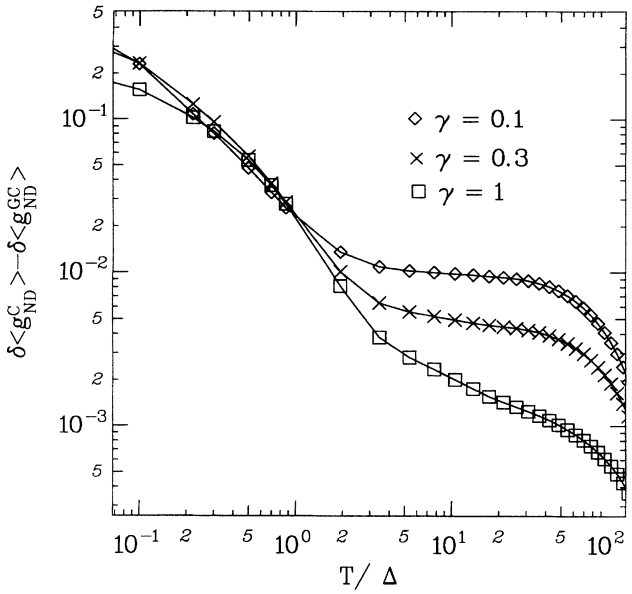

FIG. 7. Temperature dependence of the difference between the oscillating parts of $g_{\rm ND}$ in the canonical and grand canonical statistical ensembles for different values of γ. The sample studied and the range of averaging are the same as for Figs. 3 and 5.

scribed by a $1/T$ law in agreement with Ref. 32. This sharp decrease is followed by a much slower one between Δ and E_c. This behavior can be understood using the following relations:

$$\frac{\langle f_\alpha - f_\beta\rangle_N}{\epsilon_\alpha - \epsilon_\beta} = \frac{1}{\Delta} \text{ for } |\epsilon_\alpha - \epsilon_\beta| < T,$$

and

$$\frac{\langle f_\alpha - f_\beta\rangle_N}{\epsilon_\alpha - \epsilon_\beta} = \frac{\alpha - \beta}{\epsilon_\alpha - \epsilon_\beta} \text{ for } |\epsilon_\alpha - \epsilon_\beta| > T.$$

These equations yield to a γ/T dependence for $\delta g_{\rm ND}(T)$ for $\gamma < T < \Delta$.

V. DIAGONAL CONDUCTIVITY

A. Temperature and flux dependence: difference between canonical and grand canonical averages

Let us write σ_D in the following form:

$$\sigma_D = \frac{1}{V}\frac{L^2}{\gamma - i\omega}\frac{\Delta}{\Phi_0^2} g_D(\Phi), \tag{25}$$

where

$$g_D(\Phi) = -\frac{\Phi_0^2}{\Delta}\sum_\alpha \frac{\partial f_\alpha}{\partial \Phi}\frac{\partial \epsilon_\alpha}{\partial \Phi} \tag{26}$$

is a real positive quantity without dimension. g_D is related to the diagonal conductance of the system by $g_D = 2\pi \frac{G_D}{e^2/h}\frac{(\gamma - i\omega)}{\Delta}$.

1. Grand canonical ensemble

In the grand canonical case where μ is constant,

$$g_D^{\rm GC}(\Phi) = -\frac{\Phi_0^2}{\Delta}\sum_\alpha \frac{\partial f_\alpha}{\partial \epsilon}\left(\frac{\partial \epsilon_\alpha}{\partial \Phi}\right)^2. \tag{27}$$

The average value of $g_D^{\rm GC}(\Phi)$ versus chemical potential can thus be written

$$\langle g_D^{\rm GC}(\Phi)\rangle_\mu = \frac{\Phi_0^2}{\Delta^2}\langle i_\alpha^2(\Phi)\rangle, \tag{28}$$

where $i_\alpha(\Phi) = -\partial\epsilon_\alpha/\partial\Phi$ is the current carried by an electron in the state α; the averaging procedure: $\langle\cdots\rangle_\mu$ over a wide range of chemical potential compared to the temperature gives rise to a conductivity which is nearly temperature independent. It presents $\phi_0/2$-periodic oscillations whose maximum at $\phi_0/4$ is of the order of $\sigma_0\Delta/\gamma$, and thus much larger than the Drude conductance.

It is also interesting to compare our results to the analytical expression yielding the average square of the single-level persistent current from diagrammatic theory,[22] which reads

$$\langle i^2(\Phi)\rangle \simeq \left\langle\left(\frac{\partial \mu}{\partial \Phi}\right)^2\right\rangle = -2\frac{\Delta^2}{\Phi_0^2}\left(\frac{\cosh(\sqrt{2\Delta/E_c})\cos(4\pi\Phi/\Phi_0) - 1}{[\cosh(\sqrt{2\Delta/E_c}) - \cos(4\pi\Phi/\Phi_0)]^2} - \frac{1}{\cosh(\sqrt{2\Delta/E_c}) - 1}\right), \tag{29}$$

where the inverse phase coherence time has been taken equal to the level spacing. Note that the agreement between the numerical and analytical expressions is only qualitative. As we already pointed out in Sec. III, for the average current, the two quantities have a different harmonic content (see Fig. 8). Since it has been previously shown[27,29] that the harmonic content of the energy levels obtained from numerical simulations is in relatively good agreement with the results of diagrammatic theory, it is surprising to find such large disagreement concerning the harmonic content of $\langle i^2(\Phi)\rangle$. It is, however, important to note that Eq. (29) is obtained from the flux dependence of the correlation function density of states with the assumption that the harmonics λ_p of the energy levels are uncorrelated:

$$\langle \lambda_p \lambda_q\rangle = \langle \lambda_p^2\rangle \delta(p - q). \tag{30}$$

If one indeed reconstructs a fictitious quantity

$$\langle i^2(\Phi)\rangle_{\rm fict} = \sum p^2 \langle \lambda_p^2\rangle \sin^2(2\pi\Phi/\Phi_0), \tag{31}$$

according to this assumption of uncorrelated harmonics, one obtains a flux dependence which is in better agreement with Eq. (29) (see Fig. 8). In other words, this shows that Eq. (30) is not valid: the harmonics are clearly correlated.

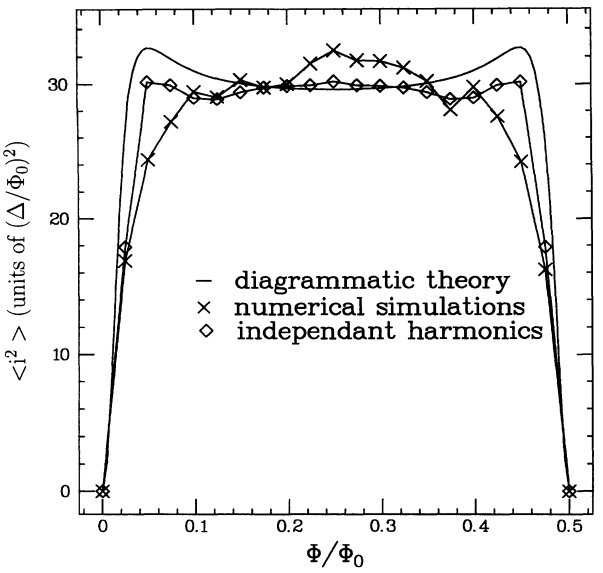

FIG. 8. Flux dependence of the average square of the single-level current obtained from numerical simulations ($64 \times 8 \times 8$, $W = 1.4$), compared with the analytical predictions of diagrammatic theory and the quantity $\langle i_{\rm fict}(\Phi)^2\rangle$ reconstructed from the flux dependence of the energy levels assuming no correlations among the different harmonics.

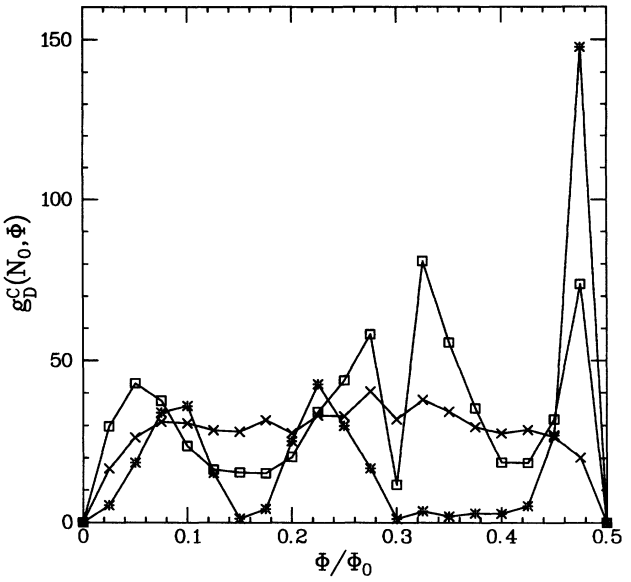

FIG. 9. Flux dependence of the canonical diagonal conductivity for a given number of electrons, for different temperatures (stars, $T = 0.2\Delta$; squares, $T \approx \Delta$; crosses, $T \approx E_c$). One notes the self-averaging effect of the temperature, $g_D^C(T = E_c) = \langle g_D^C(T = E_c)\rangle$.

2. *Canonical ensemble*

If one now considers the canonical case there is an extra term in $g(\Phi)$ which is due to the flux dependence of the chemical potential:

$$g_D^C(\Phi) = -\frac{\Phi_0^2}{\Delta}\left[\sum_\alpha \frac{\partial f_\alpha}{\partial \epsilon}\left(\frac{\partial \epsilon_\alpha}{\partial \Phi}\right)^2 - \frac{\partial \mu}{\partial \Phi}\sum_\alpha \frac{\partial f_\alpha}{\partial \epsilon}\frac{\partial \epsilon_\alpha}{\partial \Phi}\right]. \tag{32}$$

At a temperature very low compared to the average level spacing the chemical potential $\mu(N,\Phi) = \frac{1}{2}[\epsilon_N(\Phi) + \epsilon_{N+1}(\Phi)]$ lies just in the middle of the two last occupied levels, and the function $\partial f/\partial\epsilon$ is nonzero only in a window of energy width equal to T centered on $\mu(N,\Phi)$. As a result $\lim_{T\to 0}\partial f_\alpha/\partial\epsilon = 0$ for each level and $\langle g_D^C(\Phi)\rangle$ vanishes at zero temperature, in contrast with the grand canonical case. When the temperature is increased, still in the limit where $T \ll \Delta$, the flux dependence of $\langle g_D^C(\Phi)\rangle$ exhibits two spikes on each side of the values of flux where the gap at the Fermi level $\Delta_N(\Phi) = \epsilon_{N+1}(\Phi) - \epsilon_N(\Phi)$ presents a minimum lower than T. In the case of a one-dimensional spectrum these spikes occur only at $\Phi = n\Phi_0/2$, which are the only points where $\Delta_N(\Phi)$ can have a minimum. On the other hand in the case of the spectrum of a multichannel ring these spikes can take place at any value of the flux. As a result $g_D^C(N,\Phi)$ presents very strong fluctuations with N and ϕ, as illustrated by our numerical simulations depicted in Fig. 9. In the range of flux close to one of these spikes, where $\Delta_N(\Phi) > T$, it is possible to expand g_D according to

$$g_D^C(N,T,\Phi) = \frac{\Phi_0^2}{2T\Delta}\left(\frac{\partial \Delta_N}{\partial \Phi}\right)^2 \exp\left(-\frac{\Delta_N}{2T}\right). \tag{33}$$

More generally it is possible to write

$$g_D^C(N,T,\Phi) = \frac{\Phi_0^2}{\Delta^2}\left(\langle i_\alpha^2\rangle_T - \frac{(\langle i_\alpha\rangle_T)^2}{\langle 1\rangle_T}\right), \tag{34}$$

where the operation

$$\langle h_\alpha\rangle_T = \sum_\alpha \frac{\partial f_\alpha}{\partial \epsilon} h(\epsilon_\alpha)$$

defined for any function $h(\epsilon)$ becomes at high temperature equivalent to averaging this function on an energy window of width T. For $T \gg E_c$ this average is expected to be independent of T and to be equivalent to a disorder average. As a result, $\langle 1\rangle_T = 1$ and $\langle i_\alpha\rangle_{T\gg E_c} = 0$, and the conductivity becomes a self-averaging quantity which is identical to the value obtained in the grand canonical ensemble:

$$\begin{aligned} g_D^C(N, T \gg E_c, \Phi) &= \langle g_D^C(T \gg E_c, \Phi)\rangle \\ &= \langle g_D^{\rm GC}(T \gg E_c, \Phi)\rangle = \langle g_D^{\rm GC}(\Phi)\rangle \\ &= \frac{\Phi_0^2}{\Delta^2}\langle i_\alpha^2(\Phi)\rangle. \end{aligned} \tag{35}$$

The variation with temperature of $\langle g_D^C\rangle_N$ obtained from our numerical simulations is depicted in Fig. 10. The abrupt increase observed at temperatures lower than Δ is followed by a much slower one until $\langle g_D^C(T)\rangle_N$ reaches an asymptotic value which is identical with $\langle g_D^{\rm GC}\rangle$; in the temperature range $\Delta < T < E_c$ it is possible to fit the difference between $\langle g_D^{\rm GC}(T)\rangle$ and $\langle g_D^C(T)\rangle$ by the power law $T^{-1/2}$ (see Fig. 11). Note also that this temperature dependence is notably different from the one observed for the related nondiagonal quantity $\delta g_{\rm ND}^C - \delta g_{\rm ND}^{\rm GC}$ (Fig. 7).

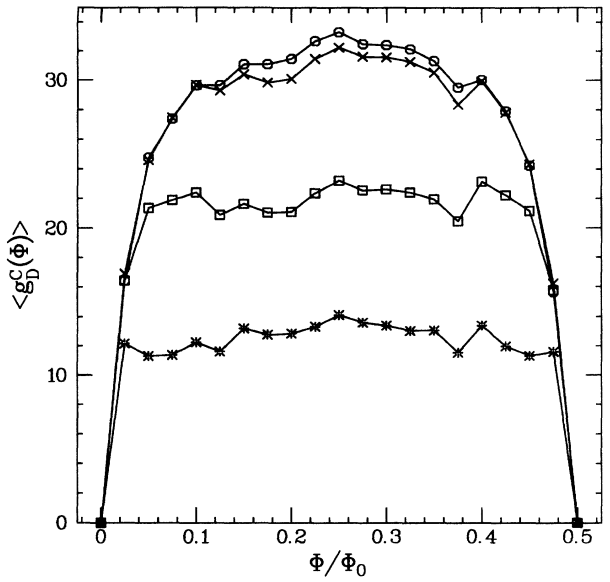

FIG. 10. Flux dependence of the canonically averaged diagonal conductance for different temperatures (stars, $T = 0.2\Delta$; squares, $T \approx \Delta$; crosses, $T \approx E_c$; circles, $T \gg E_c$).

B. Frequency dependence and imaginary conductance

The frequency dependence of $\sigma_D(\Phi)$ is given by the prefactor $(\gamma - i\omega)^{-1}$; it is thus completely determined by the ratio ω/γ; unlike the case of $\sigma_{\rm ND}$, E_c is not here a relevant energy scale. In the limit where $\omega \ll \gamma$, $\sigma_D(\Phi)$ is essentially real and proportional to $1/\gamma$; it can be also much larger than $\sigma_{\rm ND}$ which is proportional to τ_e. On the other hand in the limit where $\omega \gg \gamma$ the real part of $\sigma_D(\Phi)$ vanishes and gives rise to an imaginary contribution which adds up to the persistent current. As a result in the limit where $\omega \gg \gamma$ the imaginary conductance reads

$$\langle \mathrm{Im}(g)\rangle = -\frac{1}{\omega}\left\langle \frac{\partial I_{\rm per}}{\partial \Phi}\right\rangle + \frac{e^2}{2\pi h}\frac{\Delta}{\omega} g_D(\Phi, T). \qquad (36)$$

In the grand canonical case, $(\langle \partial I_{\rm per}/\partial\Phi\rangle)^{\rm GC} = 0$ and $\mathrm{Im}(g)^{\rm GC}_{\omega\gg\gamma} = (e^2/2\pi h)(\Phi_0^2/\Delta\omega)\langle i_\alpha^2\phi\rangle$ independent of temperature. On the other hand in the canonical case at $T = 0$, $\mathrm{Im}(g)^C = (\langle \partial I_{\rm per}/\partial\Phi\rangle)^C = \langle \partial^2 E/\partial\phi^2\rangle$. Where E is the total energy of the system, this is the old result of Kohn relating the imaginary conductivity to the stiffness of the disordered ring.[39] At higher temperature there is an extra diagonal contribution. The nonmonotonic variation with temperature of the flux-dependent part of $\langle \mathrm{Im}(\sigma)\rangle$ depicted in Fig. 12 is easily understood as resulting from the sum of the exponential decay of $\langle I_{\rm per}(T)\rangle$ and the increase of $\langle g_D^C(T)\rangle$ described above. Note that the flux dependences of $g_D(T \gg E_c)$ and of $g_{\rm per}(T = 0)$ are similar but not quite identical. Taking the derivative of Eq. (14) one can show indeed that

$$\left\langle \frac{\partial I_{\rm per}}{\partial \Phi}\right\rangle = \frac{1}{\Delta}\left[\left\langle \left(\frac{\partial \mu}{\partial \Phi}\right)^2\right\rangle + \left\langle \left(\frac{\partial^2 \mu}{\partial \Phi^2}\right)\delta\mu(\Phi)\right\rangle\right]. \qquad (37)$$

This last quantity can be identified with $\langle i^2(\Phi)\rangle - \overline{\langle i^2(\Phi)\rangle}^{\Phi}$ only if one assumes a decorrelation of the different harmonics and also of the currents bared by successive levels.

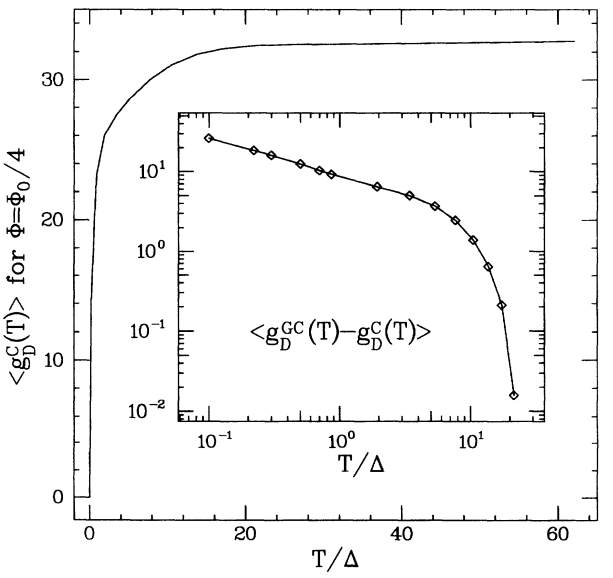

FIG. 11. Temperature dependence of the canonically averaged diagonal conductance for $\Phi = \Phi_0/4$. One notices the sharp increase from $T = 0$ to $T \approx \Delta$, the tail up to $T \approx E_c$, and the saturation at the grand canonical value for higher temperature. Inset: Difference between the grand canonically and canonically averaged diagonal conductances. This quantity decreases like $T^{-1/2}$ up to E_c, and then much faster.

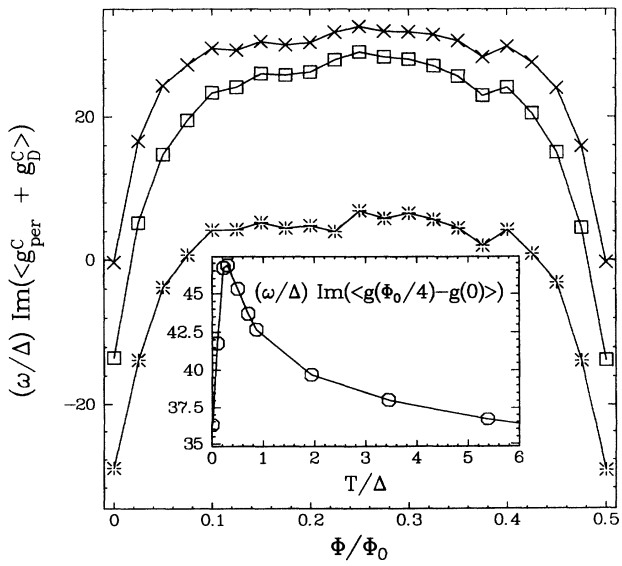

FIG. 12. Flux dependence of the imaginary part of the conductance in the canonical ensemble for different temperatures (stars, $T = 0.2\Delta$; squares, $T \approx \Delta$; crosses, $T \approx E_c$). $\langle \mathrm{Im}g^C\rangle = \langle \mathrm{Im}g^C_{\rm per}\rangle$ for $T = 0$ and $\langle \mathrm{Im}g^C\rangle \approx \langle \mathrm{Im}g^C_D\rangle$ for $T \approx E_c$. Inset: temperature dependence of the amplitude of the oscillation of the imaginary part of the conductance.

VI. THE TOTAL CONDUCTIVITY

We have seen in the preceding sections the different characteristics of the nondiagonal and diagonal components of the conductance. The flux dependence of the total conductance at zero frequency directly follows from this analysis. The grand canonical conductance is dominated by the diagonal contribution and is temperature independent. On the other hand, the canonical conductance, which is depicted in Fig. 13, depends on the temperature in the following way: at $T = 0$ it is given by only the nondiagonal contribution; its flux dependence exhibits oscillations whose signs are opposite from the grand canonical case. At nonzero temperature the diagonal contribution is added to the nondiagonal one and the sign of the flux oscillations changes, the canonical conductance becomes identical to the grand canonical one at temperatures of the order of the Thouless energy.

The frequency dependence of the total conductivity for the grand canonical ensemble, or equivalently the canonical ensemble for $T \gg E_c$, is displayed on Fig. 14 for $\Phi = 0$ and $\Phi = \Phi_0/4$. One can see that the sign of the magnetoconductance changes for $\omega > \gamma$, which corresponds to the frequency range where the diagonal contribution becomes negligible compared to the nondiagonal one. Finally, Fig. 15 summarizes the flux dependence of both real and imaginary parts of the conductance for the canonical and grand canonical statistical ensembles in the various frequency and temperature regimes. The conductance in the grand canonical ensemble is temperature

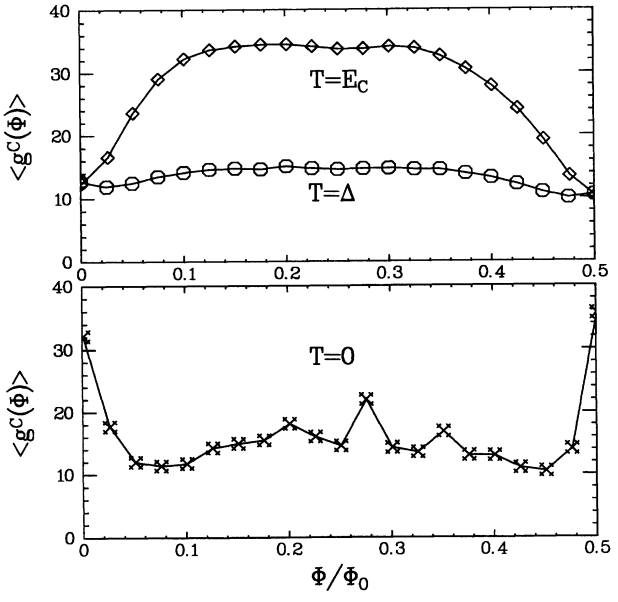

FIG. 13. Flux dependence of the total average conductance in the canonical statistical ensemble for different temperatures at zero frequency. Note the change of sign of the $\Phi_0/2$-periodic oscillations occurring at a temperature of the order of Δ. These results are obtained from numerical simulations on the Anderson model on a $30 \times 4 \times 4$ ring with disorder $W = 2$; they are averaged on the number of particles between 1/4 filling and 3/4 filling, for two different disorder configurations.

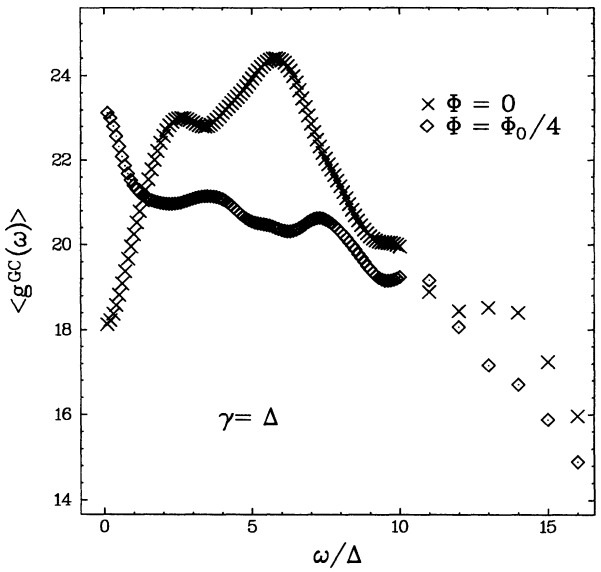

FIG. 14. Frequency dependence of the total conductance (grand canonical or canonical ensemble for $T \gg E_c$) for $\Phi = \Phi_0/4$ and $\Phi = 0$ with $\gamma = \Delta$. Note the change of sign of the magnetoconductance occurring at $\omega = \gamma$. The sample studied and the range of averaging is the same as for Figs. 3 and 5.

independent (if one neglects the variations of the parameter γ with temperature) and is identical to the canonical conductance for $T \gg E_c$. In the low-temperature regime for the canonical ensemble, the real part of the conductance is only nondiagonal and exhibits flux oscillations

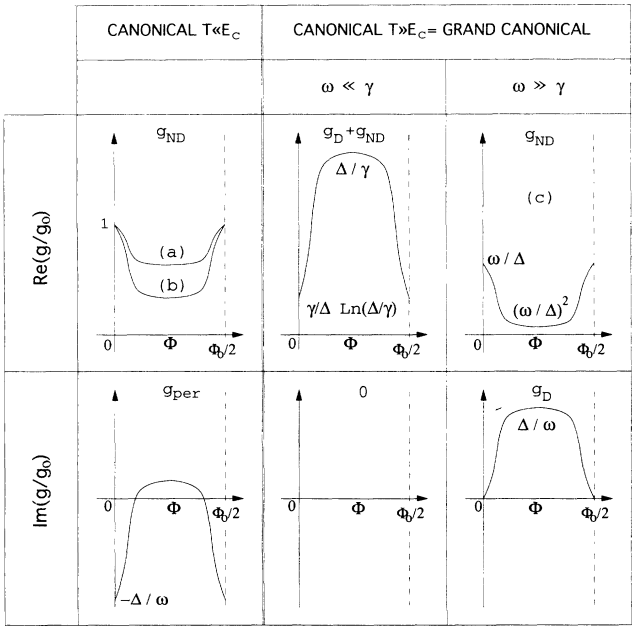

FIG. 15. Schematic summary of the flux dependences of the real and the imaginary parts of the conductivity, obtained for the different statistical ensembles for various frequency and temperature ranges. The amplitudes are given up to numerical factors. (a) $\gamma/\Delta \ln(\Delta/\gamma)$ if $\omega \ll \gamma$; (b) ω/Δ if $\gamma \ll \omega\Delta$; (c) valid only for $\omega \ll \Delta$.

whose amplitude, in the limit where both γ and ω go to zero, is of the order of the Drude conductance with a negative low-field magnetoconductance. On the other hand, for the grand canonical case at low frequency the diagonal contribution dominates the nondiagonal one and gives rise to flux oscillations of amplitude $g_0\Delta/\gamma$ with a positive low-field magnetoconductance.

The imaginary part of the conductance is proportional to the flux derivative of the average persistent current; there is no extra diagonal contribution for the canonical ensemble at zero temperature. On the other hand for the grand canonical case the average persistent current is zero but there is an extra contribution coming from the diagonal conductivity at $\omega \gg \gamma$.

VII. CONCLUSIONS

We have shown that the response function of a mesoscopic Aharonov-Bohm ring to a small time-dependent flux in the limit of a discrete spectrum presents a variety of original features and can be essentially different from the conductance of the same object connected to macroscopic measurement leads (continuous-spectrum limit). This study is relevant to the experimental situation of quantum dots made from $GaAs/Ga_{1-x}Al_xAs$ heterostructures, where recent spectroscopy studies[40] have indeed shown evidence of a discrete spectrum. We have identified different contributions to the real part of the conductance giving rise to flux oscillations of opposite sign:

(i) An off-diagonal contribution related to interlevel transitions. It is connected with the flux dependence of the level statistics.

(ii) A diagonal contribution related to the flux dependence of the occupation of the different levels. This quantity is proportional to the average square of the single-level persistent current and to the inelastic scattering time. It can be much larger than the Drude conductance.

We have emphasized the importance of the choice of the statistical ensemble: at zero temperature the canonical and grand canonical average magnetoconductances have opposite signs, and these differences persist up to temperatures of the order of the Thouless energy. These results obtained for Aharonov-Bohm geometry could easily be generalized to singly connected quantum dot geometries. We have investigated so far only the average conductance; preliminary results concerning the probability distribution of this quantity[41] show evidence of strongly non-Gaussian fluctuations different in the canonical and in the grand canonical ensembles. Such non-Gaussian fluctuations have already been predicted by Prigodin, Efetov, and Iida[42] in the tunneling conductance of quantum dots, also in the discrete-spectrum limit.

ACKNOWLEDGMENTS

This work has strongly benefited from the help and suggestions of Y. Gefen, A. Kamenev, and G. Montambaux. We also thank M. T. Beal-Monod, L. P. Lévy, and B. Spivak for fruitful discussions. Numerical simulations have been performed using Cray facilities at CCVR of Ecole Polytechnique. Laboratoire de Physique de Solides is associe an CNRS (U.A. 040002).

APPENDIX A: DETAILS OF THE COMPUTATION

The samples we studied are tori of two different shapes: a large one, of length $L_x = 64$ sites and cross section $L_y \times L_z = 8 \times 8$, and a smaller one of size $32 \times 4 \times 4$. On this lattice we numerically diagonalized the following Anderson Hamiltonian:

$$H(\Phi) = \sum_n \rho_n c_n^\dagger c_n + \sum_{n,m} (z_{n,m} c_n^\dagger c_m + \bar{z}_{n,m} c_m^\dagger c_n),$$

where $z_{n,m} = 0$ if the sites n and m are not nearest neighbors, and if they are $z_{n,m} = \exp[2i\pi\Phi/\Phi_0(x_n - x_m)/L_x]$, where x_n and x_m are the respective coordinates of sites n and m along the x axis, and where $\{\rho_n\}$ are a set of on-site energies, randomly distributed in the interval $[-\frac{W}{2}, \frac{W}{2}]$. In our case $W = 1.4$ for the bigger ring and $W = 2$ for the smaller, so that the disorder is just strong enough to make the electron motion diffusive.[27] Such a matrix can be diagonalized for different values of the magnetic flux Φ, giving rise to a set of spectra $\{\epsilon_\alpha(\Phi)\}$ and eventually a set of eigenfunctions too (we restricted the computation of eigenfunctions $|\alpha(\Phi)\rangle$ to the smallest matrix only). From the spectrum we can deduce the chemical potential $\mu(N, T, \Phi)$ for all values of the number of electrons N and the temperature T, and for the fluxes Φ for which we first diagonalized $H(\Phi)$. This is done by inverting the following implicit equation:

$$N = \sum_\alpha f_\alpha \text{ with } f_\alpha = \{\exp[\beta(\epsilon_\alpha - \mu)] + 1\}^{-1},$$

where α runs over all levels. Then we can calculate I_{per} by using Eqs. (9,14), and g_D as:

$$g_D(N, T, \Phi) = \sum_\alpha \frac{\partial f_\alpha}{\partial \epsilon} \left(\frac{\partial \epsilon_\alpha}{\partial \Phi}\right)^2 - \frac{\partial \mu}{\partial \Phi} \sum_\alpha \frac{\partial f_\alpha}{\partial \epsilon} \frac{\partial \epsilon_\alpha}{\partial \Phi} \tag{A1}$$

and

$$\frac{\partial \mu}{\partial \Phi} = \frac{\sum_\alpha \frac{\partial f_\alpha}{\partial \epsilon} \frac{\partial \epsilon_\alpha}{\partial \Phi}}{\sum_\alpha \frac{\partial f_\alpha}{\partial \epsilon}}. \tag{A2}$$

For the nondiagonal part of the conductivity according to Eq. (8) we computed the matrix elements of the kinetic momentum operator which read in the tight-binding model, $P_{\alpha\beta} = \sum_n \langle\alpha|x_n, y_n, z_n\rangle\langle x_n + 1, y_n, z_n|\beta\rangle - \langle\alpha|x_n, y_n, z_n\rangle\langle x_n - 1, y_n, z_n|\beta\rangle$, (see Fig. 16). Instead of studying a quantity for a given number of electrons or a given configuration of the disorder, it is often more

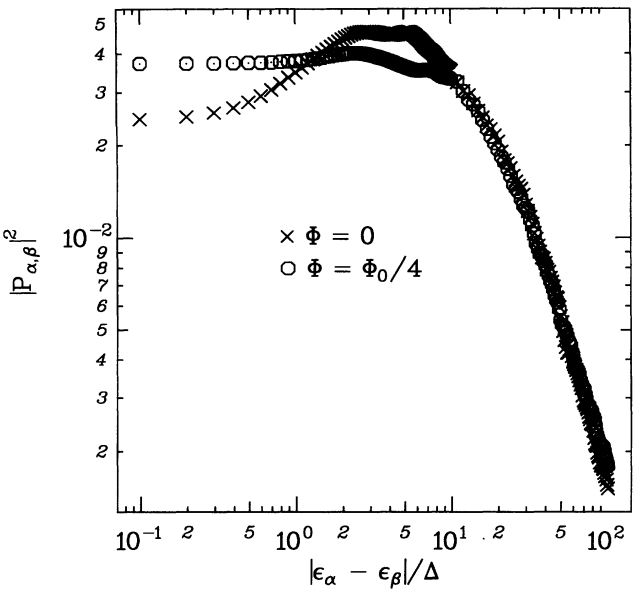

FIG. 16. Square of the matrix element of the kinetic momentum operator $|P_{\alpha\beta}|^2$ as a function of the energy difference $|\epsilon_\alpha - \epsilon_\beta|$ averaged over an energy window equal to Δ. These results are obtained from numerical simulations on the Anderson model on a $30 \times 4 \times 4$ ring with disorder $W = 2$.

interesting to compute averaged quantities. The averaging procedure involved in analytical approaches runs over the disorder, but according to the ergodicity property of mesoscopic systems in the diffusive regime, it is equivalent and numerically simpler to average over the number of electrons. The range of averaging was taken between 1/4 filling and 3/4 filling for the small sample, and between 3/8 filling and 5/8 filling for the big one.

APPENDIX B: DETERMINATION OF THE THOULESS ENERGY

In order to be able to compare our results with analytical predictions we had to estimate the Thouless energy $E_c = hD/L^2 = \frac{4}{3}Ml_e/L$. According to the empirical formula $l_e = 30/W^2$ we obtained $E_c = 20$ and $E_c = 5$ respectively for the samples $64 \times 8 \times 8$, $W = 1.4$ and $30 \times 4 \times 4$, $W = 2$. Taking this definition, the amplitude of the typical first harmonic of the total current and the average square of the single-level current are found to be

$$\langle i^2(\Phi_0/4)\rangle_{\rm num} = 1.6E_c/\Delta,$$
$$[\langle I^2_{\rm per}(\Phi_0/4)\rangle_{\rm num}]^{1/2} = 2E_c/\Delta, \tag{B1}$$

to be compared to the theoretical values:[29]

$$\langle i^2(\Phi_0/4)\rangle_{\rm th} = 2E_c/\Delta,$$
$$[\langle I^2_{\rm per}(\Phi_0/4)\rangle_{\rm th}]^{1/2} = 1.6E_c/\Delta. \tag{B2}$$

[1] L. P. Lévy, G. Dolan, J. Dunsmuir, and H. Bouchiat, Phys. Rev. Lett. **64**, 2074 (1990).
[2] V. Chandrasekhar, R. A. Webb, M. J. Brady, M. B. Ketchen, W. J. Gallagher, and A. Kleinsasser, Phys. Rev. Lett. **67**, 3578 (1991).
[3] D. Mailly, C. Chapelier, and A. Benoit, Phys. Rev. Lett. **70**, 2020 (1993).
[4] H. F. Cheung, E. K. Riedel, and Y. Gefen, Phys. Rev. Lett. **62**, 587 (1989).
[5] M. Büttiker, Y. Imry, and R. Landauer, Phys Rev. Lett. **96**, 365 (1983).
[6] R. Landauer and M. Büttiker, Phys. Rev. Lett. **54**, 2049 (1985).
[7] M. Büttiker, Ann. N.Y. Acad. Sci. **480**, 194 (1986).
[8] Y. Imry and N. S. Shiren, Phys. Rev. B **33**, 7992 (1986).
[9] N. Trivedi and D. A. Browne, Phys. Rev. B **38**, 9581 (1988).
[10] Y. Gefen and O. Entin-Wohlman, Ann. Phys. **206**, 68 (1991).
[11] B. L. Altshuler, A. G. Aronov, and B. Z. Spivak, Pis'ma Zh. Eksp. Teor. Fiz. **33**, 101 (1981) [JETP Lett. **33**, 94 (1981)].
[12] D. Y. Sharvin and Y. V. Sharvin, Pis'ma Zh. Eksp. Teor. Fiz. **34**, 285 (1981) [JETP Lett. **34**, 272 (1981)].
[13] B. Pannetier, J. Chaussy, R. Rammal, and P. Gandit, Phys. Rev. Lett. **53**, 718 (1984); Phys. Rev. B **31**, 3209 (1985).
[14] A. Kamenev, B. Reulet, H. Bouchiat, and Y. Gefen (unpublished).
[15] A. Kamenev and Y. Gefen (unpublished).
[16] C. Cohen-Tannoudji, J. Dupont-Roc, and G. Grynberg, *Processus d'interactions Entre Photons et Atomes* (Intereditions et Editions du CNRS, Paris, 1988).
[17] P. Debye, *Polar Molecules* (Chemical Catalog Co., New York, 1929), Chap. 5; J. H. Van Vleck and V. F. Weisskopf, Rev. Mod. Phys. **17**, 227 (1945).
[18] H. F. Cheung, Y. Gefen, E. K. Riedel, and W. H. Shih, Phys. Rev. **B 37**, 6050 (1988).
[19] H. Bouchiat and G. Montambaux, J. Phys. (Paris) **50**, 2695 (1989).
[20] G. Montambaux, H. Bouchiat, D. Sigeti, and R. Friesner, Phys. Rev. B **42**, 7647 (1990).
[21] Y. Imry, *Quantum Coherence in Mesoscopic Systems*, edited by B. Kramer (Plenum Press, New York, 1990), pp. 221–236.
[22] B. L. Altshuler, Y. Gefen, and Y. Imry, Phys. Rev. Lett. **66**, 88 (1991).
[23] A. Schmid, Phys. Rev. Lett. **66**, 80 (1991).
[24] D. A. Greenwood, Proc. Phys. Soc. London **71**, 585 (1958).
[25] S. F. Edwards, Philos. Mag. **3**, 1020 (1958).
[26] A. Abrikosov, L. Gor'kov, and I. Dzyaloshinski, *Methods of Quantum Field Theory in Statistical Physics* (Dover, New York, 1962).
[27] H. Bouchiat, G. Montambaux, and D. Sigeti, Phys. Rev. B

44, 1682 (1991).
[28] K. B. Efetov and S. Iida, Phys. Rev. B **47**, 15 794 (1993).
[29] E. K. Riedel and F. von Oppen, Phys. Rev. B **47**, 15 449 (1993).
[30] V. Ambegaokar and U. Eckern, Phys. Rev. Lett. **67**, 3192 (1991).
[31] L. P. Gor'kov and G. M. Eliashberg, Zh. Eksp. Teor. Fiz. **48**, 1407 (1965) [Sov. Phys. JETP **21**, 940 (1965)].
[32] B. I. Shklovskii, Pis'ma Zh. Eksp. Teor. Fiz. **36**, 287 (1982) [JETP Lett. **36**, 352 (1982)].
[33] N. F. Mott, Philos. Mag. **22**, 7 (1970).
[34] M. L. Mehta, *Random Matrices and the Statistical Theory of Energy Levels* (Academic Press, New York, 1967).
[35] K. Frahm, B. Mühlschlegel, and R. Nemeth, Z. Phys. B **78**, 91 (1990).
[36] U. Sivan and Y. Imry, Phys. Rev. B **35**, 6074 (1987).
[37] N. Dupuis and G. Montambaux, Phys. Rev. B **43**, 14 390 (1991).
[38] K. B. Efetov, Adv. Phys. **32**, 53 (1983).
[39] W. Kohn, Phys. Rev. A **133**, 171 (1964).
[40] U. Sivan, F. P. Milliken, K. Milkove, S. Rishton, Y. Lee, J. M. Hong, V. Boegli, D. Kern, and M. deFranza, Europhys. Lett. (to be published).
[41] A. Kamenev (unpublished).
[42] V. N. Prigodin, K. B. Efetov, and S. Iida, Phys. Rev. Lett. **71**, 1230 (1993).

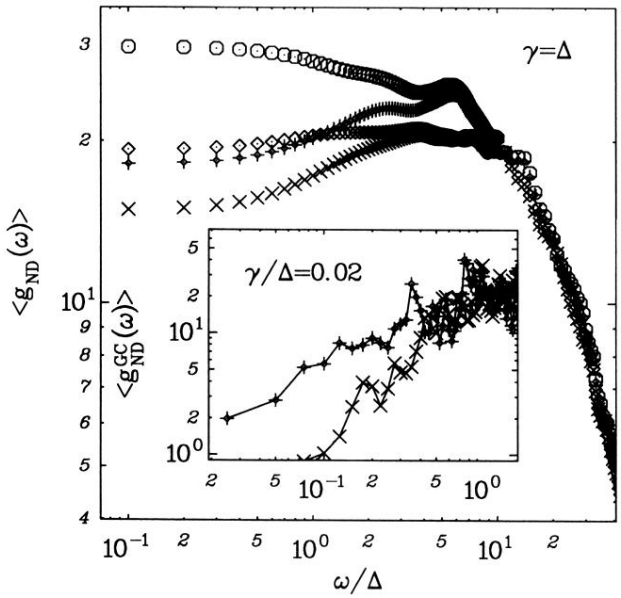

FIG. 5. Frequency dependence of the real part of the non-diagonal conductance expressed in $e^2/2\pi h$ for $\gamma = \Delta$. The canonical statistical ensemble: $\odot$, $\Phi = 0$; $\diamond$, $\Phi = \Phi_0/4$. The grand canonical statistical ensemble: $+$, $\Phi = 0$; $\times$, $\Phi = \Phi_0/4$. Note that for all cases these quantities are frequency independent below $\omega = \gamma = \Delta$. The inset shows the same quantities for $\gamma = 0.02$ and the grand canonical ensemble. In this case the ω and ω^2 dependences predicted from random matrix theory [expression (21)] are clearly observed for the low-frequency conductance at $\Phi = 0$ and $\Phi = \Phi_0/4$. The sample studied and the range of averaging is the same as for Fig. 3.

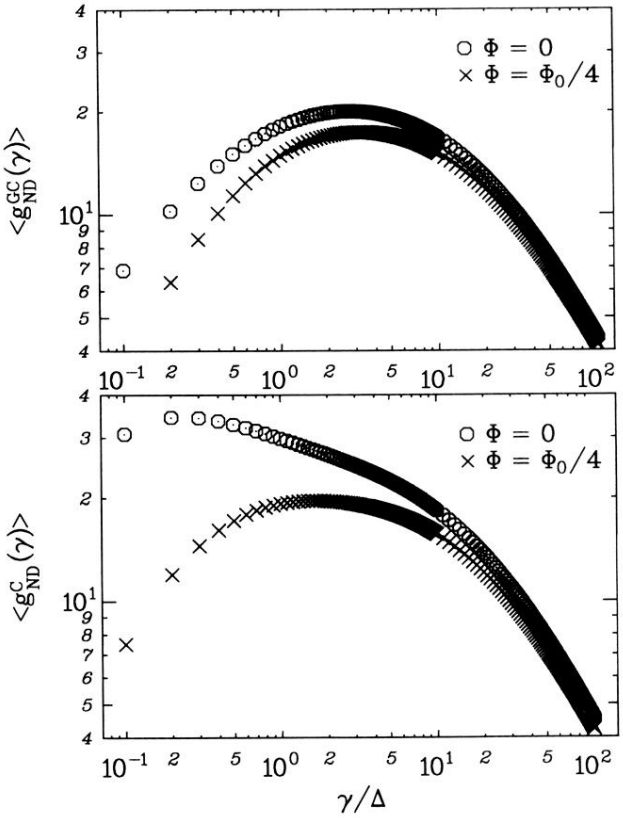

FIG. 6. γ dependence of the real part of the nondiagonal conductance at zero frequency expressed in units of $e^2/2\pi h$, for the grand canonical and canonical statistical ensembles. The sample studied and the range of averaging are the same as for Figs. 3 and 5.